Hindawi Publishing Corporation
Science and Technology of Nuclear Installations
Volume 2012, Article ID 395878, 9 pages
doi:10.1155/2012/395878

Research Article

Subcritical Multiplication Parameters of the Accelerator-Driven System with 100 MeV Protons at the Kyoto University Critical Assembly

Jae-Yong Lim, Cheol Ho Pyeon, Takahiro Yagi, and Tsuyoshi Misawa

Nuclear Engineering Science Division, Research Reactor Institute, Kyoto University, Asashiro-nishi, Kumatori-cho, Sennan-gun, Osaka 590-0494, Japan

Correspondence should be addressed to Cheol Ho Pyeon, pyeon@rri.kyoto-u.ac.jp

Received 9 November 2011; Revised 15 February 2012; Accepted 28 February 2012

Academic Editor: Piero Ravetto

Basic experiments on the accelerator-driven system (ADS) at the Kyoto University Critical Assembly are carried out by combining a solid-moderated and -reflected core with the fixed-field alternating gradient accelerator. The reaction rates are measured by the foil activation method to obtain the subcritical multiplication parameters. The numerical calculations are conducted with the use of MCNPX and JENDL/HE-2007 to evaluate the reaction rates of activation foils set in the core region and at the location of the target. Here, a comparison between the measured and calculated eigenvalues reveals a relative difference of around 10% in C/E values. A special mention is made of the fact that the reaction rate analyses in the subcritical systems demonstrate apparently the actual effect of moving the tungsten target into the core on neutron multiplication. A series of further ADS experiments with 100 MeV protons needs to be carried out to evaluate the accuracy of subcritical multiplication parameters.

1. Introduction

The accelerator-driven system (ADS) is a hybrid technique combining a reactor core and an accelerator, which has been used worldwide in research and development of nuclear transmutation of minor actinides (MAs), long-lived fission products (LLFPs), and next-generation neutron sources. In ADS, a large number of high-energy neutrons are generated directly at a heavy metal target when high-energy protons produced by the accelerator are injected onto the target. The high-energy neutrons can be utilized for maintaining nuclear fission reactions in the reactor core and achieving the purposes of the introduction of ADS. The current research on ADS involved mainly an experimental feasibility study with the use of critical assemblies and test facilities: MASURCA [1–3], YALINA-booster and -thermal [4–6], VENUS-1 [7], and the Kyoto University Critical Assembly (KUCA) [8–14]. Moreover, numerical simulations [15–20] were executed by the deterministic and stochastic approaches for the evaluation of MAs and LLFPs in ADS. The new ADS test facility of GUINEVERE [21] is being commissioned to start actual operation in subcritical states after the first critical experiments.

The Kyoto University Research Reactor Institute is pursuing an innovative research program (Kart & Lab.: Kumatori Accelerator-Driven Reactor Test Facility & Innovation Research Laboratory) to develop the fixed-field alternating gradient (FFAG) [22–24] accelerator and to establish a new neutron source by ADS in combination with KUCA and the FFAG accelerator. With the coupling of the KUCA core and the FFAG accelerator, the spallation neutrons generated by 100 MeV proton beams have been successfully injected into the uranium-loaded [25] KUCA core. In the first injection of spallation neutrons, the proton beam intensity and shape were low and poor, respectively, resulting in large statistical errors in the experiments, such as the reaction rate analyses. On the other hand, the spallation neutrons generated at the location of the tungsten target position were expected to make a reasonable contribution to neutron multiplication in the core region; however, the disadvantage of setting the target outside the core was low neutron generation in the core region by high-energy proton beams.

To resolve this drawback and enhance neutron multiplication, additional ADS experiments on the reaction rates were carried out by moving the tungsten target to another location in the subcritical core. Here, special note was taken of the effect of moving the target from the original location on subcritical multiplication parameters, including the neutron multiplication and the subcritical multiplication factor. The numerical analyses of the subcritical experiments were executed with the use of the Monte Carlo calculation code MCNPX [26] together with the nuclear data library JENDL/HE-2007 [27, 28]. The main objective of this study was to examine the accuracy of the subcritical multiplication parameters in the subcritical configurations of ADS by comparing the measured and calculated reaction rates. The preliminary (previous) experiments with high-energy neutrons generated by 100 MeV protons from the FFAG accelerator are shown in Section 2 and include descriptions of the core configuration; experimental and numerical results. The results of basic (additional) experiments on moving the target are presented in Section 3, and the conclusions are summarized in Section 4.

2. Preliminary ADS Experiments with 100 MeV Protons

2.1. Core Configuration. Among three cores designated A, B, and C at KUCA, A and B are polyethylene solid-moderated and solid-reflected cores, and C is a light water-moderated and light water-reflected one. The three cores are operated at a low mW power in the normal operating state, whereas the maximum power is 100 W. The preliminary ADS experiments were carried out in the A-core (Figure 1), which contains polyethylene reflector rods and three different fuel assemblies: normal, SV, and partial fuel assemblies (Figures 2(a), 2(b), and 2(c), resp.). The normal fuel assembly is composed of 36-unit cells and upper and lower polyethylene blocks about 591 and 537 mm long, respectively, in an aluminum sheath $54 \times 54 \times 1520\,\text{mm}^3$. For the normal and partial fuel assemblies, a unit cell in the fuel region is composed of a highly enriched uranium-aluminum fuel plate 1.59 mm (1/16″), and polyethylene plates 3.18 mm (1/8″) and 6.35 mm (1/4″). The numeral 14 corresponds to the number of fuel plates in the partial fuel assembly used to reach the criticality mass. The horizontal dimensions of all fuel and polyethylene plates are $5.08 \times 5.08\,\text{mm}^2$ (2″ × 2″).

The tungsten target located outside the core is not easily moved to the center of the core because control and safety rods are fixed in the core and function as the control driving system. The neutron guide composed of several shielding materials, including iron (Fe), boron (B), polyethylene, the beam duct, and a special fuel assembly with a void (SV, Figure 2(b)), are installed. In the neutron guide, the role of the SV assemblies is to direct the highest number possible of the high-energy neutrons generated in the target to the center of the fuel region, in order to improve neutron multiplication. Moreover, to collimate the high-energy neutrons, it was necessary to reduce the thermal component moderated in the reflector region before their reaching the fuel region. This reduction was achieved by shielding unnecessary fast neutrons and by capturing parasite thermal neutrons. For deflecting unnecessary fast neutrons, the close vicinity in front of the target included the Fe block around the guide void to shield the fast neutrons from inelastic scattering. For capturing parasite thermal neutrons, polyethylene blocks containing 10 wt% B around the guide void were set around the Fe shielding near the target and in the two rows next to the assemblies. The rest of the neutron guide consisted of polyethylene assemblies and one void space. Details of the neutron guide were as described in [8, 9]. 100 MeV protons generated from the accelerator were injected into a subcritical system with the following parameters: 10 pA beam intensity; 30 Hz repetition rate; 100 ns pulsed width; 1.0×10^6 1/*s* neutron yield.

2.2. Experimental Analyses. In the subcritical experiments, gold (^{197}Au) and indium (^{115}In) foils were selected as normalization factors for monitoring reactor power in the core and neutron source generation at the target, respectively. The difference between the normalization factors in the core and at the target was attributable to the sensitivity of the thermal neutrons and the high-energy neutrons, respectively. The reaction rates of the ^{115}In wire (1.5 mm diameter and 750 mm long) in the core and the ^{115}In foil ($10 \times 10 \times 1\,\text{mm}^3$) at the target were normalized by those of the ^{197}Au foil (8 mm diameter and 0.05 mm thick) emitted by $^{197}\text{Au}(n, \gamma)^{198}\text{Au}$ reactions attached in the core center (O, 15; Figure 1), and of the ^{115}In foil emitted by $^{115}\text{In}(n, n')^{115\text{m}}\text{In}$ reactions attached at the original location of the target, respectively. The experimental error in each activation foil was estimated to be about 5%, including the statistical error of γ-ray counts and the full width at half maximum (FWHM) of the γ-ray spectrum peak. The experiments were carried out within subcriticality level 770 pcm ($0.77\%\Delta k/k$). Here, the subcritical state was attained by the full insertion of C1, C2, and C3 control rods and the full withdrawal of S4, S5 and S6 safety rods (Figure 1). The measured subcriticality was obtained from the combination of both the control and safety rod worth by the rod drop method and its calibration curve by the positive period method. In the KUCA core, the subcriticality was attained by the full insertion of all control and safety rods within 2,000 pcm ($0.20\%\Delta k/k$; $k_{\text{eff}} = 0.98$), and the representative subcriticality level around 3,000 pcm is achieved by the removal of fuel rods in the ADS experiments. When the representative subcriticality is obtained, as a result, the change in the core characteristics, including the control rod worth, the neutron flux shape and the neutron spectrum, is apparently observed in comparison with before and after the removal of fuel rods. Therefore, the ADS experiments were carried out within the subcritical level attained by inserting the control and safety rods to maintain the core characteristics from the viewpoint of reactor physics.

The effect of the subcritical multiplication parameters was evaluated by thermal neutron flux distribution estimated through the horizontal measurement of $^{115}\text{In}(n, \gamma)^{116\text{m}}\text{In}$ reaction rates by activation analysis of the In wire. The wire was set in an aluminum guide tube within the 3 mm

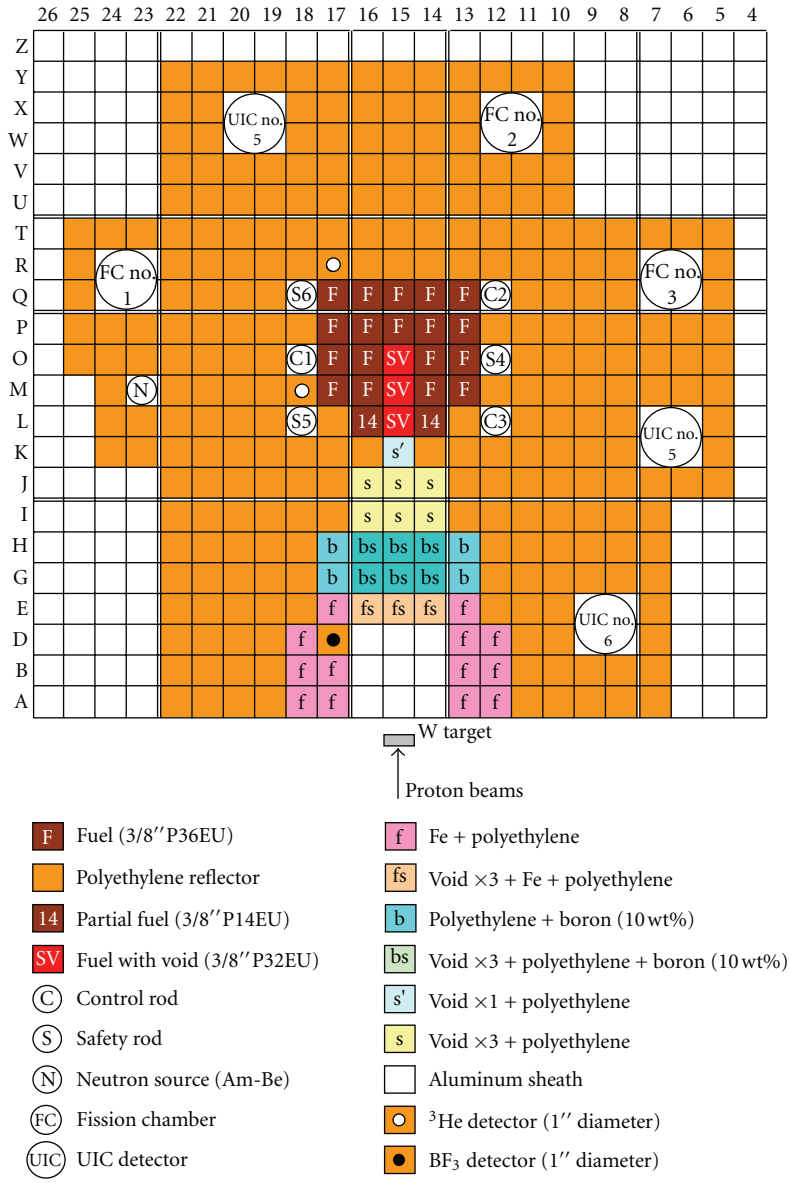

Figure 1: Top view of the KUCA A-core (A3/8″P36EU(3)) in the ADS experiments.

gap between rows 13 and 14 (Figure 1), from the front of the tungsten target to the center of the fuel region (13-14, A–P; Figure 1), at the height of the axial center of the fuel assembly. For comparison between the experiment and the calculation, normalization was based on reactor power: the ^{197}Au$(n, \gamma)^{198}$Au reaction rate set in the center of the core was measured. A global experimental error of about 5% was considered significant on reaction rate measurements of the In wire.

The subcriticality calculations were executed with the use of the Monte Carlo multiparticle transport code, MCNPX, in combination with nuclear data library JENDL/HE-2007. The irradiation foils and the In wire were included in the simulated geometry and transport calculation because the effects of their reactivity are not negligible; reaction rates were deduced from tallies taken in the reaction rate experiments. Although better in the core region, an overall statistical error of 5% remained in the reaction rate in the present results. The results of eigenvalue calculations were obtained after 1,000 active cycles of 50,000 histories each. The deduced subcriticalities had statistical errors of 10 pcm (0.01%$\Delta k/k$). The fixed-source calculations were executed by a total of 1.0×10^8 histories, which led to a statistical error of less than 5% in the reaction rates.

The results of measured and calculated subcriticalities are presented in Table 1. A comparison between the experiments and the calculations demonstrated the ability of MCNPX calculations to reproduce the subcriticality level to within 2% of the C/E (calculation/experiment) value. A comparison made of the measured and the calculated reaction rate distributions to validate the calculation method demonstrated that the calculated reaction rate distribution

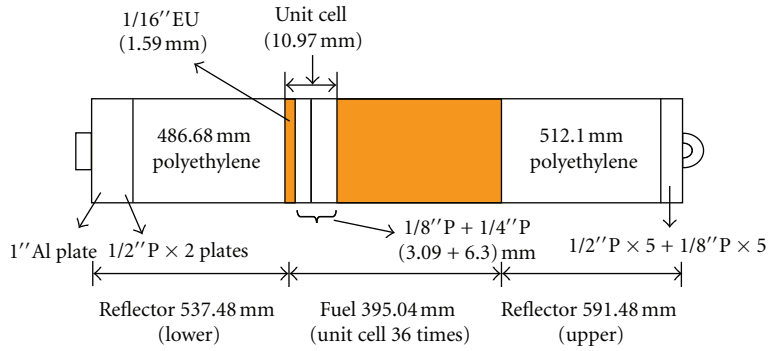

(a) 3/8P″36EU fuel assembly (F; Figure 1)

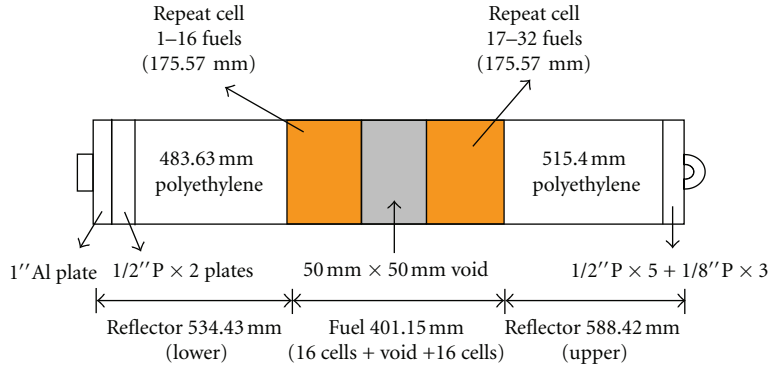

(b) 3/8P″32EU fuel assembly (SV; Figure 1)

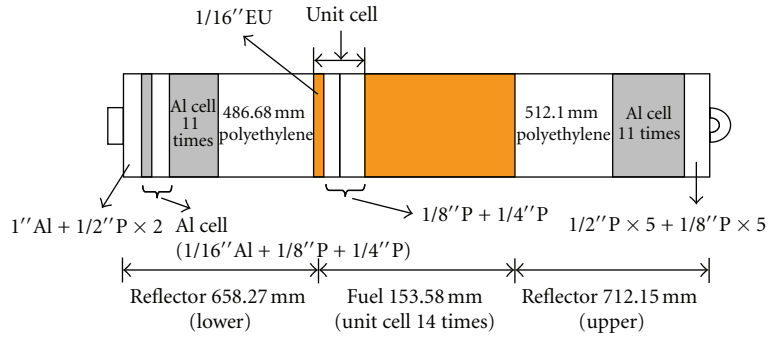

(c) 3/8P″14EU fuel assembly (14; Figure 1)

Figure 2: Schematic drawing of fuel assemblies in the A-core.

Table 1: Comparison between the measured and calculated subcriticalities obtained from the experiments (Figure 1) and calculations (MCNPX with JENDL/HE-2007).

Calculation (pcm)	Experiment (pcm)	C/E
773	760	1.02

(Figure 3) agreed approximately with the experimental one within the statistical errors in the experiments; however, the experimental errors were considerably larger than those of the calculations. These larger errors were attributable to the status of the proton beams, including the weak beam intensity and the poor beam shape at the target.

3. Basic ADS Experiments with 100 MeV Protons

The neutron spectrum analyses were conducted numerically for investigating anticipated high-energy neutrons at each location for the injection of the high-energy protons before the basic experiments, as shown in Figure 4. The high-energy neutrons were attained in front of target location (A, 15) and were dominant over the region of a few MeV neutrons of energy. The further the distance was from the tungsten target, including locations (E, 15), (J, 15), and (O, 15), the more thermalized the neutron spectrum is: this fact demonstrated that the high-energy neutrons generated at the location of the original target should be little affected upon neutron multiplication in the core, and the thermal neutrons

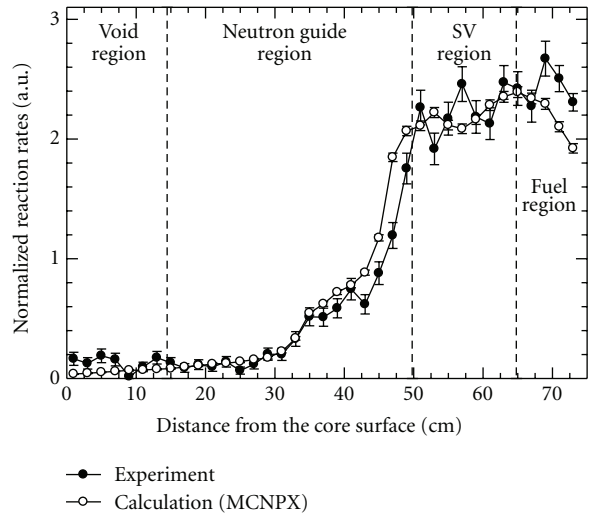

Figure 3: Comparison between the measured and calculated reaction rates of ^{115}In$(n, \gamma)^{116m}$In reactions along the region of (13-14, A–P; Figure 1).

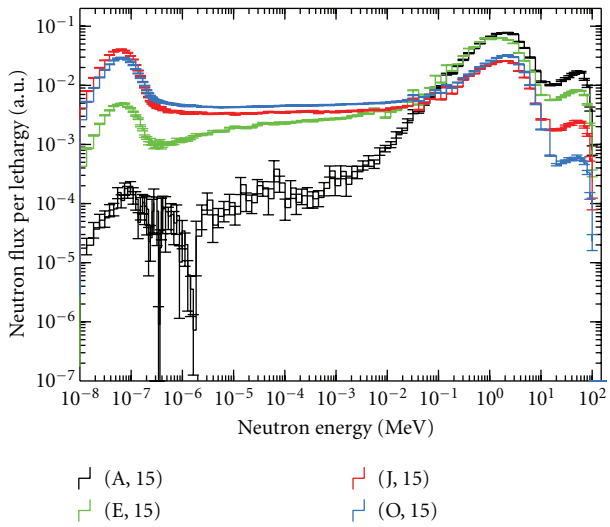

Figure 4: Comparison between neutron spectra at four points in the ADS experiments (Figure 1).

moderated in the reflector region were compared to be less than other locations.

For optimizing the effect of moving the target from its original location, additional experiments were carried out in the same core (Figure 5) as in a previous study described in Section 2: the composition of the neutron guide was made partly of lead (Pb) instead of Fe, thereby attaining neutron multiplication around the target region by the injection of high-energy neutrons into the shielding material, Pb. Also, the effect of moving the target was investigated through analyses of neutron multiplication, as in the previous study [29] at KUCA. In the experiments, the ^{115}In$(n, \gamma)^{116m}$In reaction rates were measured in the core region, and neutron multiplication was deduced by the reaction rate distribution, when the tungsten target was moved from the original location to another one close to the core center. Finally

Table 2: Comparison between the measured and calculated subcriticalities obtained from the experiments (Figure 5) and calculations (MCNPX with JENDL/HE-2007).

Case	Calculation (pcm)	Experiment (pcm)	C/E
(A, 15)	706	772	0.91
(G, 15)	659	737	0.89
(K, 15)	674	740	0.91

the actual effect of moving the target was examined by comparing the experimental and numerical analyses. As in Section 3, the experiments were carried out around subcriticality level 750 pcm ($0.75\%\Delta k/k$), and subcriticality was attained and then measured. Notably, the 100 MeV protons generated from the accelerator were injected into a subcritical system under the following parameters: 30 pA beam intensity; 30 Hz repetition rate; 200 n*s* pulsed width; 1.0×10^7 1/*s* neutron yield.

3.1. Subcriticality. The numerical calculations were executed with the use of MCNPX together with the JENDL/HE-2007 library. The numerical evaluation of subcriticality by JENDL/HE-2007 was in agreement with experimental data and within a relative difference of 10% (Table 2), whereas the accuracy of eigenvalue calculations was not good compared with the previous analyses presented in Section 2. By MCNPX, the eigenvalue calculations were executed for 5,000 active cycles of 10,000 histories. The subcriticalities in the eigenvalue calculations had statistical errors within 10 pcm ($0.01\%\Delta k/k$). Since the reactivity effects of activation foils and wire in the core are not negligible, they were included in the simulated geometry and transport calculations.

3.2. Reaction Rate Distribution. The calculated reaction rate was obtained by evaluating the volume tallies of activation foils. The statistical error of the reaction rates in the fixed-source calculations was within 5% after a total of 1.0×10^8 histories. The difference in the experimental results along region (13-14, A–P; Figure 5) is shown in Figure 6(a), by changing the location of the tungsten target to another one: in front of the original target (A, 15); between the target and the core (G, 15); in front of the fuel region (K, 15). From the experimental results in Figure 6(a), the reaction rate distribution was observed to be high in the SV and fuel regions, when the tungsten target was set at location (G, 15), although the core configuration of reaction rates varied in the SV and fuel regions. Comparison of the experimental and numerical results revealed the approximate reconstruction of the ^{115}In$(n, \gamma)^{116m}$In reaction rates by MCNPX with JNEDL/HE-2007 shown in Figure 6(b), whereas the discrepancy was found to be in some regions of (G, 15) by the difference in experimental results in the core configuration.

3.3. Neutron Multiplication and Subcritical Multiplication Factor. Neutron multiplication M and subcritical multiplication factor k_s were experimentally and numerically analyzed on the basis of the accuracy in Section 3.2, related to

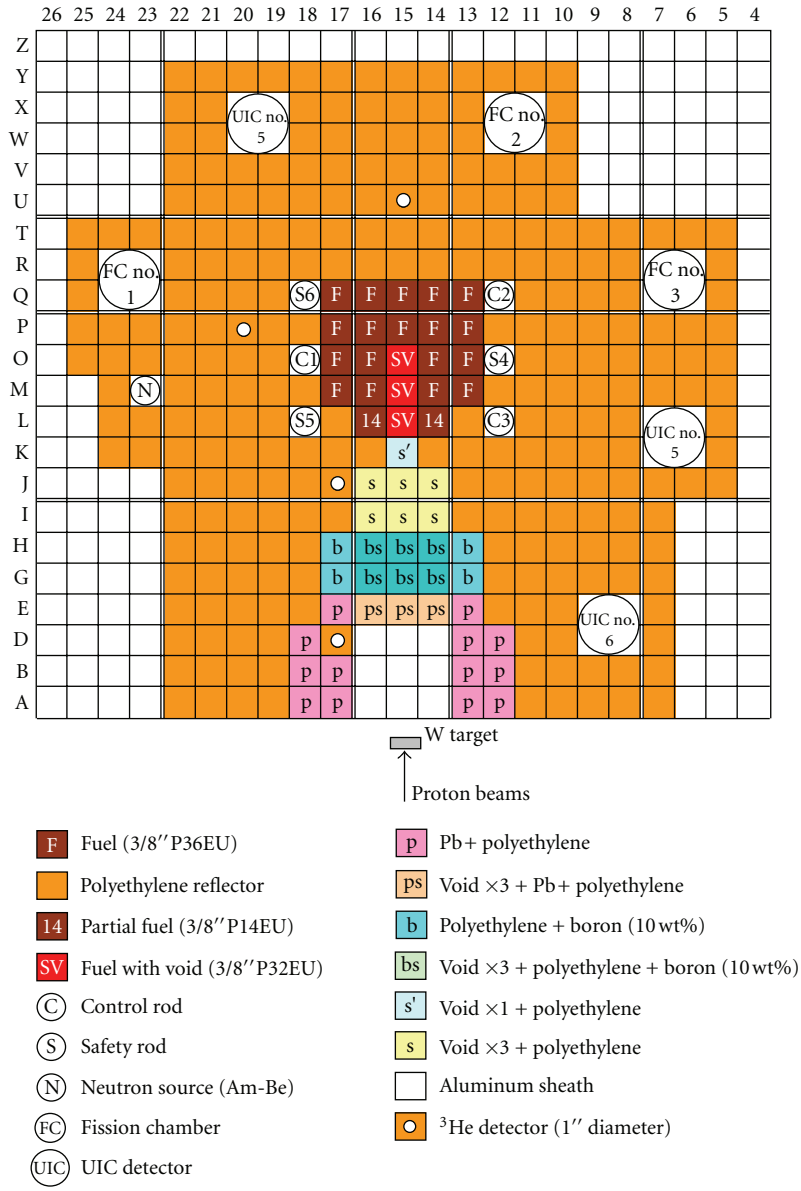

Figure 5: Top view of the KUCA A-core (A3/8″P36EU(3)) in the ADS experiments.

the subcritical multiplication parameters. The methodology of the theoretical basis used was as briefly described [29].

In the ADS study on the subcritical system, the neutron multiplication M is defined as the ratio of total fission neutrons F and the external neutron source rates S, to the rate of external neutron source as follows:

$$M = \frac{F + S}{S}. \tag{1}$$

The neutron multiplication M is also expressed by the subcritical multiplication factor k_s, which is defined as the ratio of the fission neutrons to the total neutrons in the system by the fission and source neutrons as follows:

$$M = \frac{1}{1 - k_s}. \tag{2}$$

In (1) and (2), k_s can be expressed by F and S as follows:

$$k_s = \frac{F}{F + S}. \tag{3}$$

Assuming that the fission reaction rate F is independent of one-dimensional (x-direction) in the thermal neutron field, the total fission neutrons can be expressed approximately by the In reaction rates R_{In} of $^{115}\mathrm{In}(n, \gamma)^{116\mathrm{m}}\mathrm{In}$ reactions as follows:

$$\begin{aligned} F &= \int_V \int_0^\infty \nu\Sigma_f(\underline{r}, E)\phi_s(\underline{r}, E)d\underline{r}\,dE \\ &\approx \int_a R_{\mathrm{In}}(x, y_0, z_0)dx, \end{aligned} \tag{4}$$

where V indicates the whole volume in the system, ν the average number of fission neutrons per fission reaction, Σ_f

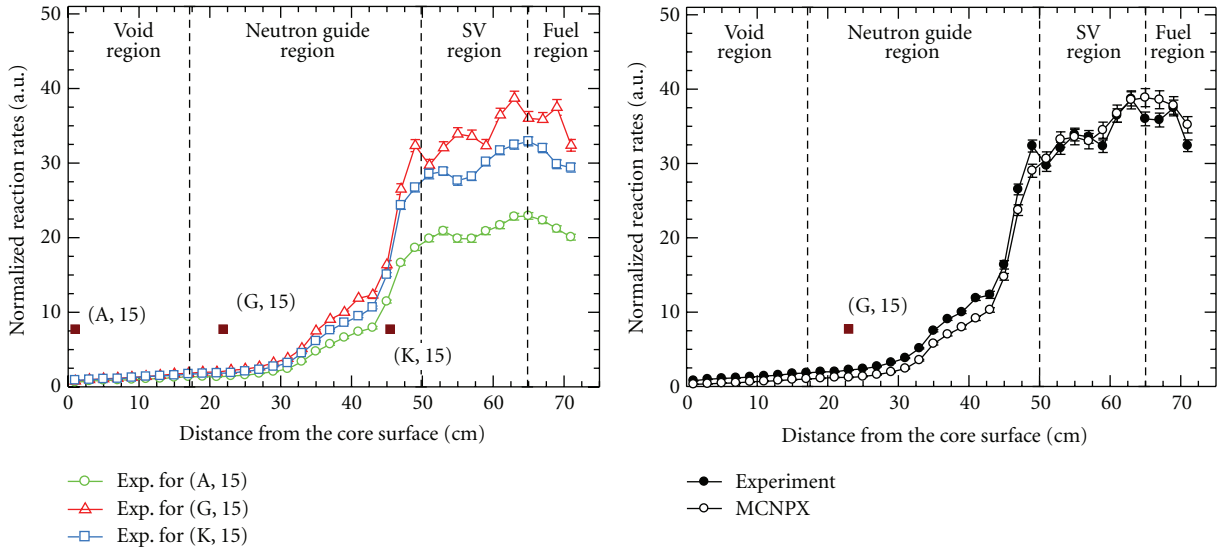

(a) experimental results for moving the tungsten target

(b) comparison between the measured and calculated reaction rates for the location (G, 15) of tungsten target

FIGURE 6: Reaction rates of $^{115}\mathrm{In}(n, \gamma)^{116\mathrm{m}}\mathrm{In}$ reactions along the region (13-14, A–P; Figure 2) in the ADS experiments.

the fission cross-section, ϕ_s the neutron flux at position $\underline{r}$ with energy E in the presence of an external source, and a the In wire along the fuel regions (SV and fuel regions; Figure 5) in the core. The external neutron source rate S can be expressed approximately by the In reaction rates $R_{\mathrm{In}'}$ of $^{115}\mathrm{In}(n, n')^{115\mathrm{m}}\mathrm{In}$ reactions in the same manner as that of (4) as follows:

$$S = \int_V \int_0^\infty s(\underline{r}, E) d\underline{r}\, dE \approx \int_{r_s} R_{\mathrm{In}'}(\underline{r}) d\underline{r}, \quad (5)$$

where $s(\underline{r}, E)$ indicates the external neutron source rates at position $\underline{r}$ with energy E, and r_s the position of external neutron source. The validity of approximation and the applicability of the methodology mentioned above have already been demonstrated in the previous study [29].

Finally, using (4) and (5), the neutron multiplicationr M and subcritical multiplication factor k_s in (1) and (3), respectively, can be expressed approximately as follows:

$$M \approx \frac{\int_a R_{\mathrm{In}}(x, y_0, z_0) dx}{\int_{r_s} R_{\mathrm{In}'}(\underline{r}) d\underline{r}} + 1, \quad (6)$$

$$k_s \approx \frac{\int_a R_{\mathrm{In}}(x, y_0, z_0) dx}{\int_a R_{\mathrm{In}}(x, y_0, z_0) dx + \int_{r_s} R_{\mathrm{In}'}(\underline{r}) d\underline{r}}. \quad (7)$$

The measured reaction rates of the In wire (1.5 mm diameter and 750 mm long) emitted by $^{115}\mathrm{In}(n, \gamma)^{116\mathrm{m}}\mathrm{In}$ reactions in the core were normalized by those of the $^{197}\mathrm{Au}$ foil (8 mm diameter and 0.05 mm thick) emitted by $^{197}\mathrm{Au}(n, \gamma)^{198}\mathrm{Au}$ reactions attached at the core center (O, 15; Figure 5), and the reaction rates of the In foil ($10 \times 10 \times 1\,\mathrm{mm}^3$) emitted by $^{115}\mathrm{In}(n, n')^{115\mathrm{m}}\mathrm{In}$ reactions at moving the target were normalized by those of the $^{115}\mathrm{In}$ foil ($10 \times 10 \times 1\,\mathrm{mm}^3$) emitted by $^{115}\mathrm{In}(n, n')^{115\mathrm{m}}\mathrm{In}$ reactions attached at the original location of the target. The experimental error in each activation foil was estimated to be about 5%, including the statistical error of γ-ray counts and FWHM of the γ-ray spectrum peak. The calculated reaction rates of the In wire and the Au foil in the core were included in the simulated geometry and transport calculations and deduced from tallies taken in the fixed-source calculations. Also the calculated reaction rates of the In foil at the target was obtained by the same manner of the previous fixed source calculations, modeling the proton injection on the tungsten target.

The C/E value of the experiments and calculations of fission and source terms in (4) and (5), respectively, is shown in Table 3. Comparing with absolute values, the accuracy of fission term was within a relative difference of 20%, and that of the source term was well within the allowance for experimental error. The discrepancy between the measured and the calculated fission terms was caused mainly by the uncertainties of experimental values obtained from the reaction rates of the In wire especially in locations (G, 15) and (K, 15), because locations (G, 15) and (K, 15) were far from that of original target, and the proton weak and poor beams were in intensity and shape, respectively. As a result, it was considered that the In wire was not sufficiently activated to obtain the information on the thermal neutrons. As shown in Table 4, the neutron multiplication was considered to involve a large discrepancy caused by the evaluation of the C/E values of fission and source terms; inversely, the subcritical multiplication factor was considered fairly good in the evaluation of C/E values. The constant values of the measured and the calculated k_s demonstrated that the source term was not contributed largely to that of k_s, since the external source was located outside the core: the values of M and k_s in (1) and (2), respectively, were remarkably

Table 3: Comparison between the measured and calculated fission and source terms obtained from the experiments (Figure 5) and calculations (MCNPX with JENDL/HE-2007).

	Fission term F			Source term S		
Case	Calculation	Experiment	C/E	Calculation	Experiment	C/E
(A, 15)	46.37 ± 1.51	43.53 ± 0.27	1.07	0.04 ± 0.01	0.02 ± 0.01	1.70
(G, 15)	77.05 ± 2.50	67.34 ± 0.38	1.14	0.01 ± 0.01	0.02 ± 0.01	0.53
(K, 15)	68.55 ± 2.26	55.81 ± 0.29	1.23	0.03 ± 0.01	0.03 ± 0.01	1.14

Table 4: Comparison between the measured and calculated neutron multiplication and subcritical multiplication factor obtained from the experiments (Figure 5) and calculations (MCNPX with JENDL/HE-2007).

	Neutron multiplication M		
Case	Calculation	Experiment	C/E
(A, 15)	$(1.15 \pm 0.04) \times 10^3$	$(1.83 \pm 0.05) \times 10^3$	0.63
(G, 15)	$(6.25 \pm 0.21) \times 10^3$	$(2.88 \pm 0.09) \times 10^3$	2.17
(K, 15)	$(2.04 \pm 0.09) \times 10^3$	$(1.88 \pm 0.05) \times 10^3$	1.08
	Subcritical multiplication factor k_s		
Case	Calculation	Experiment	C/E
(A, 15)	0.99913 ± 0.00003	0.99945 ± 0.00001	1.00
(G, 15)	0.99984 ± 0.00003	0.99965 ± 0.00001	1.00
(K, 15)	0.99951 ± 0.00003	0.99947 ± 0.00001	1.00

dependent on that of F in (4), because of the location of the target outside the core. While the accuracy of the neutron multiplication was attributable to the experimental variation of reaction rates of the In wire, the actual effect of setting the tungsten target at location (G, 15) was found to be more significant than setting the target in the original location.

4. Conclusions

The ADS experiments with 100 MeV protons were carried out at KUCA to evaluate the subcritical multiplication parameters using the reaction rates. Comparison of the results of the experiments and the calculations by MCNPX with JENDL/HE-2007 revealed the following.

In the first injection experiments, the subcriticality C/E values of the experiments and the calculations were in fairly good agreement within a relative difference of 2%, and the calculated reaction rate distribution reconstructed the experimental one, although the proton beams were observed to be weak in intensity and poor in shape at the target. In the basic experiments, the notable effect of moving the target from the original location was clearly revealed in the analyses of the subcritical multiplication parameters for attaining further neutron multiplication in the core.

Further ADS study at KUCA needs to be conducted to investigate experimentally the effect of the subcritical multiplication parameters presented in this study, when the subcriticality and the neutron spectrum are varied. The present experimental data could be conducive to basic research of ADS, such as the verification of precision in numerical analyses by stochastic and deterministic approaches.

Acknowledgments

This work was supported by the "Energy Science in the Age of Global Warming" of the Global Center of Excellence (G-COE) program (J-051) of the Ministry of Education, Culture, Sports, Science and Technology of Japan. The authors are grateful to all the technical staff and students of KUCA for their assistance during the experiments.

References

[1] R. Soule, W. Assal, P. Chaussonnet et al., "Neutronic studies in support of accelerator-driven systems: the MUSE experiments in the MASURCA facility," *Nuclear Science and Engineering*, vol. 148, no. 1, pp. 124–152, 2004.

[2] M. Plaschy, C. Destouches, G. Rimpault, and R. Chawla, "Investigation of ADS-Type heterogeneities in the MUSE4 critical configuration," *Journal of Nuclear Science and Technology*, vol. 42, no. 9, pp. 779–787, 2005.

[3] J. F. Lebrat, G. Aliberti, A. D'Angelo et al., "Global results from deterministic and stochastic analysis of the MUSE-4 experiments on the neutronics of accelerator-driven systems," *Nuclear Science and Engineering*, vol. 158, no. 1, pp. 49–67, 2008.

[4] C. M. Persson, A. Fokau, I. Serafimovich et al., "Pulsed neutron source measurements in the subcritical ADS experiment YALINA-Booster," *Annals of Nuclear Energy*, vol. 35, no. 12, pp. 2357–2364, 2008.

[5] Y. Gohar, G. Aliberti, I Bolshinsky et al., "YALINA-booster subcritical assembly conversion," *Transactions of American Nuclear Society*, vol. 101, pp. 39–40, 2009.

[6] M. Tesinsky, C. Berglöf, T. Bäck et al., "Comparison of calculated and measured reaction rates obtained through foil activation in the subcritical dual spectrum facility YALINA-Booster," *Annals of Nuclear Energy*, vol. 38, no. 6, pp. 1412–1417, 2011.

[7] H. H. Xia, "The progress of researches on ADS in China," *ICFA Beam Dynamics Newsletter*, vol. 49, pp. 72–80, 2009.

[8] C. H. Pyeon, Y. Hirano, T. Misawa et al., "Preliminary experiments on accelerator-driven subcritical reactor with pulsed neutron generator in Kyoto university critical assembly," *Journal of Nuclear Science and Technology*, vol. 44, no. 11, pp. 1368–1378, 2007.

[9] C. H. Pyeon, M. Hervault, T. Misawa, H. Unesaki, T. Iwasaki, and S. Shiroya, "Static and kinetic experiments on accelerator-driven system with 14 MeV neutrons in Kyoto University Critical Assembly," *Journal of Nuclear Science and Technology*, vol. 45, no. 11, pp. 1171–1182, 2008.

[10] C. H. Pyeon, H. Shiga, K. Abe et al., "Reaction rate analysis of nuclear spallation reactions generated by 150, 190, and 235 MeV protons," *Journal of Nuclear Science and Technology*, vol. 47, no. 11, pp. 1090–1095, 2010.

[11] C. H. Pyeon, H. Shiga, T. Misawa, T. Iwasaki, and S. Shiroya, "Reaction rate analyses for an accelerator-driven system with 14 MeV neutrons in the Kyoto university critical assembly," *Journal of Nuclear Science and Technology*, vol. 46, no. 10, pp. 965–972, 2009.

[12] H. Taninaka, K. Hashimoto, C. H. Pyeon, T. Sano, T. Misawa, and T. Ohsawa, "Determination of lambda-mode eigenvalue separation of a thermal accelerator-driven system from pulsed neutron experiment," *Journal of Nuclear Science and Technology*, vol. 47, no. 4, pp. 376–383, 2010.

[13] H. Taninaka, K. Hashimoto, C. H. Pyeon et al., "Determination of subcritical reactivity of a thermal accelerator-driven system from beam trip and restart experiment," *Journal of Nuclear Science and Technology*, vol. 48, no. 6, pp. 873–879, 2011.

[14] H. Taninaka, A. Miyoshi, K. Hashimoto et al., "Feynman-α analysis for a thermal subcritical reactor system driven by an unstable 14 MeV neutron source," *Journal of Nuclear Science and Technology*, vol. 48, no. 11, pp. 1272–1280, 2011.

[15] K. Tsujimoto, T. Sasa, K. Nishihara, H. Oigawa, and H. Takano, "Neutronics design for lead-bismuth cooled accelerator-driven system for transmutation of minor actinide," *Journal of Nuclear Science and Technology*, vol. 41, no. 1, pp. 21–36, 2004.

[16] T. Sasa, H. Oigawa, K. Tsujimoto et al., "Research and development on accelerator-driven transmutation system at JAERI," *Nuclear Engineering and Design*, vol. 230, no. 1–3, pp. 209–222, 2004.

[17] T. Sugawara, T. Iwasaki, T. Chiba, and K. Nishihara, "Development of dynamics code and proposal of start-up procedure for accelerator driven system," *Journal of Nuclear Science and Technology*, vol. 43, no. 1, pp. 20–31, 2006.

[18] K. Nishihara, K. Iwanaga, K. Tsujimoto, Y. Kurata, H. Oigawa, and T. Iwasaki, "Neutronics design of accelerator-driven system for power flattening and beam current reduction," *Journal of Nuclear Science and Technology*, vol. 45, no. 8, pp. 812–822, 2008.

[19] T. Sugawara, K. Nishihara, K. Tsujimoto, T. Sasa, and H. Oigawa, "Analytical validation of uncertainty in reactor physics parameters for nuclear transmutation systems," *Journal of Nuclear Science and Technology*, vol. 47, no. 6, pp. 521–530, 2010.

[20] T. Sugawara, M. Sarotto, A. Stankovskiy, and G. Van Den Eynde, "Nuclear data sensitivity/uncertainty analysis for XT-ADS," *Annals of Nuclear Energy*, vol. 38, no. 5, pp. 1098–1108, 2011.

[21] W. Uyttenhove, P. Baeten, G. Van Den Eynde, A. Kochetkov, D. Lathouwers, and M. Carta, "The neutronic design of a critical lead reflected zero-power reference core for on-line subcriticality measurements in accelerator driven systems," *Annals of Nuclear Energy*, vol. 38, no. 7, pp. 1519–1526, 2011.

[22] M. Tanigaki, K. Takamiya, H. Yoshino, N. Abe, T. Takeshita, and A. Osanai, "Control system for the FFAG complex at KURRI," *Nuclear Instruments and Methods in Physics Research A*, vol. 612, no. 2, pp. 354–359, 2010.

[23] T. Planche, E. Yamakawa, T. Uesugi et al., "Scaling FFAG rings for rapid acceleration of muon beams," *Nuclear Instruments and Methods in Physics Research A*, vol. 622, no. 1, pp. 21–27, 2010.

[24] T. Planche, J.-B. Lagrange, E. Yamakawa et al., "Harmonic number jump acceleration of muon beams in zero-chromatic FFAG rings," *Nuclear Instruments and Methods in Physics Research A*, vol. 632, no. 1, pp. 7–17, 2011.

[25] C. H. Pyeon, T. Misawa, J. Y. Lim et al., "First injection of spallation neutrons generated by high-energy protons into the kyoto university critical assembly," *Journal of Nuclear Science and Technology*, vol. 46, no. 12, pp. 1091–1093, 2009.

[26] J. S. Hendricks, G. W. McKinney, L. S. Waters et al., *MCNPX User's Manual, Version 2.5.0*, LA-UR-05-2675, Los Alamos National Laboratory, 2005.

[27] T. Fukahori, "JENDL high-energy file," *Journal of Nuclear Science and Technology*, vol. 2, supplement, pp. 25–30, 2002.

[28] H. Takada, K. Kosako, and T. Fukahori, "Validation of JENDL high-energy file through analyses of spallation experiments at incident proton energies from 0.5 to 2.83 GeV," *Journal of Nuclear Science and Technology*, vol. 46, no. 6, pp. 589–598, 2009.

[29] H. Shahbunder, C. H. Pyeon, T. Misawa, and S. Shiroya, "Experimental analysis for neutron multiplication by using reaction rate distribution in accelerator-driven system," *Annals of Nuclear Energy*, vol. 37, no. 4, pp. 592–597, 2010.